THE JOURNAL OF BIOLOGICAL CHEMISTRY
Vol. 277, No. 33, Issue of August 16, pp. 29386–29398, 2002
Printed in U.S.A.

ETS-1 Transcription Factor Binds Cooperatively to the Palindromic Head to Head ETS-binding Sites of the Stromelysin-1 Promoter by Counteracting Autoinhibition*

Received for publication, January 4, 2002, and in revised form, April 22, 2002
Published, JBC Papers in Press, May 28, 2002, DOI 10.1074/jbc.M200088200

David Baillat‡, Agnès Bègue, Dominique Stéhelin, and Marc Aumercier§

From the CNRS Unité Mixte de Recherche 8526, Institut de Biologie de Lille, Institut Pasteur de Lille, B.P. 447, 1 Rue Calmette, 59021 Lille Cedex, France

Stromelysin-1 (matrix metalloproteinase-3) is a member of the matrix metalloproteinase family. Regulation of its gene expression is critical for tissue homeostasis. Patterns of increased co-expression of stromelysin-1 and ETS-1 genes have been observed in pathological processes. Stromelysin-1 promoter is transactivated by ETS proteins through two palindromic head to head ETS-binding sites, an unusual configuration among metalloproteinase promoters. By using surface plasmon resonance, electrophoretic mobility shift assay, and photocross-linking, we showed that full-length human ETS-1 (p51) binds cooperatively to the ETS-binding site palindrome of the human stromelysin-1 promoter, with facilitated binding of the second ETS-1 molecule to form an ETS-1·DNA·ETS-1 ternary complex. The study of N-terminal deletion mutants allowed us to conclude that cooperative binding implied autoinhibition counteraction, requiring the 245–330-residue region of the protein that is encoded by exon VII of the gene. This region was deleted in the natural p42 isoform of ETS-1, which was unable to bind cooperatively to the palindrome. Transient transfection experiments showed a good correlation between DNA binding and promoter transactivation for p51. In contrast, p42 showed a poorer transactivation, reinforcing the significance of cooperative binding for full transactivation. It is the first time that ETS-1 was shown to be able to counteract its own autoinhibition.

Stromelysin-1 (matrix metalloproteinase-3) is a member of the matrix metalloproteinase family with a wide spectrum of substrates. It plays a crucial role in extracellular matrix remodeling during normal processes such as tissue morphogenesis, growth, and wound repair (1, 2). A tight regulation of its gene expression is critical for tissue homeostasis. Indeed, its misregulation is associated with pathologic conditions such as rheumatoid and osteoarthritis (3, 4), Alzheimer's disease (5), tumor invasiveness, and metastasis (6–8). In addition, it was recently reported (9, 10) that stromelysin-1 by itself promoted mammary carcinogenesis in a mouse model system. Stromelysin-1 expression is mainly controlled at the transcription level. A number of specific DNA elements in the human stromelysin-1 promoter have been shown to be important in the regulation of its transcription (11, 12). Among them, two palindromic ETS-binding sites (EBS)[1] with a 5′-GGA(A/T)-3′ core motif at −216 to −209 and at −208 to −201 bind ETS transcription factors. This EBS palindrome is required for basal expression and 12-*O*-tetradecanoylphorbol-13-acetate tumor promoter response (13) and is highly conserved through species.

The ETS-1 oncoprotein, the founding member of the ETS family, transactivates the rat stromelysin-1 promoter through this palindrome (14). These family members are important transcription factors involved in development (15–18). They have also been implicated in several types of cancer and other human diseases (19). All ETS proteins share a conserved ~85-amino acid DNA binding domain (ETS domain) organized into a winged helix-turn-helix motif (20).

Their specificity for target promoters is controlled at several levels. Nevertheless, DNA binding modulation can be viewed as the first transcriptional control. Binding specificity to a given EBS can be partially provided by the flanking sequences surrounding the EBS core. Further specificity occurs through combinatorial interactions of ETS proteins with co-factors at adjacent DNA elements (21, 22). Additional control is provided by autoinhibition (23). This phenomenon, mediated by cis-acting inhibitory modules, negatively regulates DNA binding through intramolecular interactions. ETS-1 represents the best studied example (24–26). Its autoinhibition can be counteracted by interaction with protein partners (27–31) resulting in a cooperative binding of each molecule.

Given that on one hand the same pro-inflammatory factors as interleukin-1β and tumor necrosis factor α are able to activate stromelysin-1 and ETS-1 (32, 33) and on the other hand that patterns of increased co-expression of these both genes have been shown in processes such as rheumatoid arthritis (34), glomerulonephritis (35), angiogenesis (36), and tumor invasion (37), there is a strong presumption that misregulation of stromelysin-1 could be mediated by ETS-1.

Previous work (13, 14) showed that both EBS of the palindrome acted synergistically to transactivate stromelysin-1 gene promoter. Nevertheless, in a heterologous system ETS-1 and ETS-2 showed no cooperative binding to the palindrome (14). In contrast, other studies proved that the functional EBS palin-

* This work was supported in part by Grant ARC 5601 from the Association pour la Recherche sur le Cancer (to M. A.). The costs of publication of this article were defrayed in part by the payment of page charges. This article must therefore be hereby marked "*advertisement*" in accordance with 18 U.S.C. Section 1734 solely to indicate this fact.

‡ Recipient of a BDI (Bouvse de Docteur Ingénieur) fellowship from the CNRS and Région Nord-Pas de Calais.

§ To whom correspondence should be addressed. Tel.: 33-3-20-87-10-97; Fax: 33-3-20-87-11-11; E-mail: marc.aumercier@ibl.fr.

[1] The abbreviations used are: EBS, ETS-binding site; CBF, core binding factor; SPR, surface plasmon resonance; M1, mutant site 1; M2, mutant site 2; M1M2, mutant sites 1 and 2; DR, direct repeat; IP, inverted palindrome; EMSA, electrophoretic mobility shift assay; DTT, DL-dithiothreitol; CaMKII, calmodulin-dependent protein kinase II; $Ru(bpy)_3Cl_2$, ruthenium(II) tris-bipyridyl dichloride; RU, resonance unit; DBD, DNA binding domain; WT, wild type; DR, direct repeat; ERG, ETS-related gene.

TABLE I
Sequences of stromelysin-1 promoter, wild type, and mutants

The EBS core sequences are represented as boldface letters in the sequence. → and ← represent the EBS in both possible orientations, and × designates a mutated EBS.

Name	Sequences	EBS topology
WT	5'----ACCAAGACA**GGAA**GCAC**TTCC**TGGAGATTA---- 3'	→ ←
M1	5'----ACCAAGACAAAAAGCAC**TTCC**TGGAGATTA---- 3'	× ←
M2	5'----ACCAAGACA**GGAA**GCACTTTTTGGAGATTA---- 3'	→ ×
DR	5'----ACCAAGACA**GGAA**GCCA**GGAA**GTGAGATTA---- 3'	→ →
IP	5'----ACCAAGAGC**TTCC**TGCA**GGAA**GTGAGATTA---- 3'	← →
WT+4	5'----ACCAAGACA**GGAA**GCACGCAC**TTCC**TGGAGATTA---- 3'	→ ←
M1M2	5'----ACCAAGACAAAAAGCACTTTTTGGAGATTA---- 3'	× ×

dromes present in GATA-1 and p53 promoter (38, 39) cooperatively bound ETS-1 and ETS-2.

Given the growing importance of the EBS palindrome for the transcriptional regulation of stromelysin-1 by ETS proteins (40–42), we reinvestigated the binding of ETS-1 to the stromelysin-1 promoter.

In this study, by using surface plasmon resonance (SPR), electrophoretic mobility shift assay (EMSA), and photo-cross-linking experiments, we show that the full-length human ETS-1 protein (p51) binds with a positive cooperativity to the EBS palindrome of the human stromelysin-1 promoter. This cooperativity is seen exclusively under a palindromic topology and leads to the formation of a ternary ETS-1·DNA·ETS-1 complex. By using kinetic analysis and N-terminal deletion mutants, we conclude that the observed cooperativity is because of a facilitated binding of the second ETS-1 molecule to form the ternary ETS-1·DNA·ETS-1 complex. Furthermore, this mechanism implies autoinhibition counteracting of ETS-1 through the 245–330-residue region of the protein encoded by the exon VII of the gene. The p42 isoform of ETS-1, lacking only this region, is unable to bind cooperatively to the palindrome, despite a better binding to each EBS. Transient transfection experiments show for p51 a good correlation between DNA binding and promoter transactivation. In contrast, p42 shows a poorer transactivation reinforcing the significance of cooperative binding for a full ETS-1-mediated transactivation of the promoter. To our knowledge, this is the first time that ETS-1 is shown to be able to counteract its own autoinhibition.

MATERIALS AND METHODS

Site-directed Mutagenesis—Mutant forms of the human stromelysin-1 promoter corresponding to M1, M2, M1M2, DR, and IP were generated by site-directed mutagenesis using appropriate oligonucleotides (Table I) and the QuickChange Site-directed Mutagenesis kit (Stratagene®) with a pØGH plasmid (HGH-TGES, Nichols Institute Diagnostics) containing the −1303/+4 fragment of the wild type human stromelysin-1 promoter as a template (13).

Luciferase Reporter Gene Constructions—Fragments −478/+4 of the wild type and mutated human stromelysin-1 promoters were excised from the pØGH vector by *Xba*I and *Bam*HI endonuclease digestion. Fragments were blunted with T4-DNA polymerase and cloned into the *Sma*I site of the pGL3 basic vector (Promega). Correct insertion and orientation were confirmed by sequencing.

Bacterial Expression Vector Constructions—Human full-length ETS-1 and 5′ deletion mutant constructions were obtained by PCR amplification using appropriate primers (Table II) and cloning into a pTyb2 vector (T7 Impact System, New England Biolabs). The human ETS-1 cDNA inserted in a pSG5 vector was used as a template. The 5′ primers were always designed in-frame with the *Nde*I site. The amplified fragments were submitted to *Nde*I digestion and cloned into a pTyb2 vector, previously digested by *Nde*I and *Sma*I endonucleases. The ETS-1 p42 isoform construct was obtained by PCR site-directed mutagenesis (43), resulting in the large deletion of the exon VII. All constructs were checked for nucleotide sequence before expression.

Eukaryotic Expression Vector Construction—The human ETS-1 cDNA inserted in a pSG5 vector already existed (42). The ETS-1 p42 isoform cDNA cloned in pSG5 vector was obtained by the same way as for the pTyb2 cloning.

Generation of Biotinylated Oligonucleotides for SPR Experiments—The 99-bp biotinylated double-stranded DNA fragments were obtained by PCR amplification using 5′-biotinyl-GAATTCCAGTCAATTTTTC-CAG-3′ as a forward primer and 5′-CAAGGCAACACAGTGATTA-ATC-3′ as a reverse primer. Amplified fragments were purified on QIAquick columns (Qiagen) and checked for sequence before immobilization on the Sensor Chip.

Expression and Purification of ETS-1 Proteins—Proteins were purified using the T7-Impact System (New England Biolabs). *Escherichia coli* (ER2566) was transformed with the appropriate recombinant plasmid. Fresh overnight cultures were diluted 1:25 in 250 ml of Luria-Bertani medium and incubated at 37 °C with shaking at 230 rpm. When culture density reached A_{595nm} = 0.7, isopropyl-β-D-thiogalactopyranoside was added to a final concentration of 0.3 mM. The culture was incubated at 30 °C with shaking for 3–4 h. Cultures were harvested, and pellets were washed with phosphate-buffered saline and suspended in 10 ml of lysis buffer (50 mM Tris, pH 8, 150 mM NaCl, 1 mM EDTA, 0.1% (v/v) Triton X-100, complete protease inhibitors mixture (Complete™, Roche Molecular Biochemicals)). Bacteria were lysed with a French press using a 1000 pounds/square inch pressure. Lysates were clarified by a 5-min centrifugation at 20,000 × *g* at 4 °C followed by a subsequent 15-min centrifugation at 20,000 × *g* at 4 °C. Each clarified lysate was applied to a 5-ml chitin bead column (New England Biolabs). Columns were washed with 20 volumes of column buffer (lysis buffer without protease inhibitors) and rapidly flushed with 3 volumes of elution buffer (column buffer without Triton X-100) containing 50 mM dithiothreitol (DTT) (Roche Molecular Biochemicals). Columns were then stored 16 h at 4 °C for peptidic cleavage. Proteins were eluted by 15 ml of elution buffer in 1-ml fractions. Fractions with proteins were pooled, and for further purification were diluted and chromatographed on a Mono S HR 5/5 column (Amersham Biosciences) equilibrated with 10 mM Tris, pH 8, 50 mM NaCl, 1 mM DTT, and 0.5 mM phenylmethylsulfonyl fluoride using a Bio-Rad Biologic Chromatography System (Bio-Rad). Proteins were eluted by a NaCl gradient (0.05–1 M). Fractions containing the protein were quick-frozen by immersion in liquid nitrogen and stored at −80 °C after dialysis against HBS-EP (0.01 M Hepes, pH 7.4, 0.15 M NaCl, 3 mM EDTA, 0.005% (v/v) polysorbate 20). Yields were measured by colorimetry (Bio-Rad protein assay) and corrected by comparison against known protein standards (bovine serum albumin) on SDS-PAGE after Coomassie Blue staining.

Electrophoretic Mobility Shift Assay—Double-stranded synthetic oligonucleotides corresponding to the WT, M1, M2, WT + 4, and M1M2 mutants of the stromelysin-1 (−223/−194) promoter region (Table I) were end-labeled using T4 polynucleotide kinase and [γ-^{32}P]ATP and were subsequently purified by electrophoresis on a 20% polyacrylamide gel in TBE buffer (90 mM Tris borate, 1 mM EDTA). Recombinant proteins (4 pmol) were incubated with 0.5 ng of probe in 20 μl of binding reaction buffer (20 mM Tris, pH 7.9, 80 mM NaCl, 1 mM EDTA, 2 mM

TABLE II

PCR primers used for cloning the human ETS-1 N-terminal deletion mutants

Forward Primers[a]	
ΔN45	5'-AAGTAT**CATATG**ATGTCTCAAGCATTAAAAGC-3'
ΔN144	5'-AAGTAT**CATATG**GGAGTCAACCCAGCCTATCC-3'
ΔN245	5'-AAGTAT**CATATG**AAACTCGGGGGCCAGGAC-3'
ΔN280	5'-AAGTAT**CATATG**GTTCCCTCCTATGACAGCTTCG-3'
ΔN301	5'-AAGTAT**CATATG**AAGGGCACCTTCAAGGAC-3'
ΔN331	5'-AAGTAT**CATATG**GGCAGTGGACCAATCCAG-3'
Reverse Primer[b]	
	5'-CCCCTCGTCGGCATCTGGCTTGAC-3'

[a] Forward primers were designed in frame with *Nde*I site (bold letters). The six additional 5′ bases were introduced to enable *Nde*I digestion.
[b] The same reverse primer was used for all PCR amplifications.

TABLE III

Schematic representation of the kinetic models and the related differential equations

A corresponds to the analyte (ETS-1) and B to the ligand (DNA). A_2B stands for a ternary complex composed of one ligand and two analyte molecules. A_2B^* depicts the same ternary complex but in a rearranged form. The concentration of X is represented by $[X]$.

M1 model, one-to-one interaction	
$A + B \Leftrightarrow AB$ (k_{a1}; k_{d1}; K_{d1})	$d[B]/dt = -k_{a1}[A][B] + k_{d1}[AB]$
	$d[AB]/dt = k_{a1}[A][B] - k_{d1}[AB]$
WT model A, two independent and non-equivalent binding sites on ligand	
$A + B \Leftrightarrow AB$ (k_{a1}; k_{d1}; K_{d1})	$d[B]/dt = -k_{a1}[A][B] + k_{d1}[AB] - k_{a2}[A][B] + k_{d2}[BA]$
$A + B \Leftrightarrow BA$ (k_{a2}; k_{d2}; K_{d2})	$d[AB]/dt = k_{a1}[A][B] - k_{d1}[AB] - k_{a2}[A][AB] + k_{d2}[A_2B]$
$A + AB \Leftrightarrow A_2B$ (k_{a2}; k_{d2}; K_{d2})	$d[BA]/dt = k_{a2}[A][B] - k_{d2}[BA] - k_{a1}[A][BA] + k_{d1}[A_2B]$
$A + BA \Leftrightarrow A_2B$ (k_{a1}; k_{d1}; K_{d1})	$d[A_2B]/dt = k_{a2}[A][AB] - k_{d2}[A_2B] + k_{a1}[A][BA] - k_{d1}[A_2B]$
WT model B, two independent binding sites on ligand and conformational change	
$A + B \Leftrightarrow AB$ (k_{a1}; k_{d1}; K_{d1})	$d[B]/dt = -k_{a1}[A][B] + k_{d1}[AB] - k_{a2}[A][B] + k_{d2}[BA]$
$A + B \Leftrightarrow BA$ (k_{a2}; k_{d2}; K_{d2})	$d[AB]/dt = k_{a1}[A][B] - k_{d1}[AB] - k_{a2}[A][AB] + k_{d2}[A_2B]$
$A + AB \Leftrightarrow A_2B$ (k_{a2}; k_{d2}; K_{d2})	$d[BA]/dt = k_{a2}[A][B] - k_{d2}[BA] - k_{a1}[A][BA] + k_{d1}[A_2B]$
$A + BA \Leftrightarrow A_2B$ (k_{a1}; k_{d1}; K_{d1})	$d[A_2B]/dt = k_{a2}[A][AB] - k_{d2}[A_2B] + k_{a1}[A][BA] - k_{d1}[A_2B] - k_{a3}[A_2B] + k_{d3}[A_2B^*]$
$A_2B \Leftrightarrow A_2B^*$ (k_{a3}; k_{d3}; K_{d3})	$d[A_2B^*]/dt = k_{a3}[A_2B] - k_{d3}[A_2B^*]$
WT model C, sequential binding	
$A + B \Leftrightarrow AB$ (k_{a1}; k_{d1}; K_{d1})	$d[B]/dt = -k_{a1}[A][B] + k_{d1}[AB]$
$A + AB \Leftrightarrow A_2B$ (k_{a2}; k_{d2}; K_{d2})	$d[AB]/dt = k_{a1}[A][B] - k_{d1}[AB] - k_{a_2}[A][AB] + k_{d2}[A_2B]$
	$d[A_2B]/dt = k_{a2}[A][AB] - k_{d2}[A_2B]$
WT model D, sequential binding and conformational change	
	$d[B]/dt = -k_{a1}[A][B] + k_{d1}[AB]$
$A + B \Leftrightarrow AB$ (k_{a1}; k_{d1}; K_{d1})	$d[AB]/dt = k_{a1}[A][B] - k_{d1}[AB] - k_{a2}[A][AB] + k_{d2}[A_2B]$
$A + AB \Leftrightarrow A_2B$ (k_{a2}; k_{d2}; K_{d2})	$d[A_2B]/dt = k_{a2}[A][AB] - k_{d2}[A_2B] - k_{a3}[A_2B] + k_{d3}[A_2B]$
$A_2B \Leftrightarrow a_2B^*$ (k_{a3}; k_{d3}; K_{d3})	$d[A_2B^*]/dt = k_{a3}[A_2B] - k_{d3}[A_2B^*]$

DTT, 10% glycerol) for 30 min on ice. Complexes formed were resolved on a 5% polyacrylamide (acrylamide/bisacrylamide 29:1, Euromedex) non-denaturing gel in 0.25× TBE buffer at room temperature. Gels were dried and autoradiographed at −80 °C.

Kination Assay—Recombinant human ETS-1 p51 (4 pmol) was phosphorylated by incubation with 150 units of calmodulin-dependent protein kinase II (CaMKII, rat truncated recombinant protein, New England Biolabs) at 30 °C for various times in 20 μl of kination buffer (20 mM Tris, pH 7.5, 10 mM $MgCl_2$, 0.5 mM DTT, 0.1 mM EDTA, 2 mM $CaCl_2$, 2.4 μM calmodulin, 100 μM ATP) in the presence of [γ-^{32}P]ATP. The reaction was stopped by addition of 20 μl of 2× gel loading buffer (0.1 M Tris, 4% SDS, 1.44 M β-mercaptoethanol, 20% glycerol, 0.2% xylene cyanol, and 0.2% bromphenol blue) and subsequent boiling for 2 min. Samples were resolved by SDS-PAGE, and gels were dried and quantified using a PhosphorImager (Amersham Biosciences). For gel shift assays, the recombinant proteins (4 pmol) were phosphorylated under the same conditions for 90 min in absence of radioactive ATP. Subsequent binding reactions were performed with 0.5 ng of ^{32}P-labeled probe. The volume was adjusted to 30 μl with binding reaction buffer.

Cross-linking Experiments—Cross-linking reactions were carried out in a total volume of 20 μl in phosphate-buffered saline solution (Invitrogen). 4 pmol of ETS-1 were incubated with various amounts of ^{32}P-labeled oligonucleotides (0.125 to 2 ng) for 30 min on ice. $Ru(bpy)_3Cl_2$ (Aldrich) and ammonium persulfate were added to 150 μM and 2.5 mM, respectively, just before illumination by standard flashlight at a distance of 10 cm. Then the samples were immediately quenched with 20 μl of 2× gel loading buffer and heated to 100 °C for 2 min. Complexes were resolved by electrophoresis through a 10% SDS-polyacrylamide gel. Gel were dried and autoradiographed at −80 °C.

SPR Binding Assay—SPR measurements were carried out using a BIAcore 2000 apparatus (Biacore®). Double-stranded biotinylated oligonucleotides (99 bp long) were immobilized on a streptavidin-coupled CM5 Sensor Chip using standard protocol as indicated in the Amine Coupling Kit (Biacore®). HBS-EP BIA certified buffer (0.01 M Hepes, pH 7.4, 0.15 M NaCl, 3 mM EDTA, 0.005% (v/v) polysorbate 20, Biacore®) was used as a running buffer. Briefly, flow rate was fixed at 10 μl/min. Streptavidin was injected at 500 ng/μl in 10 mM sodium acetate, pH 3.5, for 12 min. Biotinylated double-stranded oligonucleotides were injected through each flow cell at 200 ng/ml onto the Sensor Chip until a suitable stable RU signal was obtained. The integrity and quantity of fixed DNA was checked by a 120-s injection of 1.6 μM calf histone H1 (Sigma) at 10 μl/min. Equilibrium binding experiments were carried out at 25 °C using a flow rate of 10 μl/min. Proteins were injected at the desired concentration in HBS-EP for 120 s. The Sensor Chip was regenerated by a 60-s injection of 0.03% SDS. Final curves were obtained by subtraction of the signal corresponding to a flow cell functionalized with M1M2 oligonucleotide. Resonance units (RU) for calculation of the binding ratios were measured at the end of the injection when binding equilibrium was reached.

SPR Kinetic Assay—Kinetic experiments were carried out at 15 °C at a flow rate of 30 μl/min on a CM5 Sensor Chip prepared as described above with a 100-RU stable fixation of each biotinylated double-stranded oligonucleotide. ETS-1 p51 isoform was injected using the KINJECT procedure for 90 s at 7.25, 14.5, 29, and 58 nM concentrations. Dissociation of the complex was then monitored for 300 s before regen-

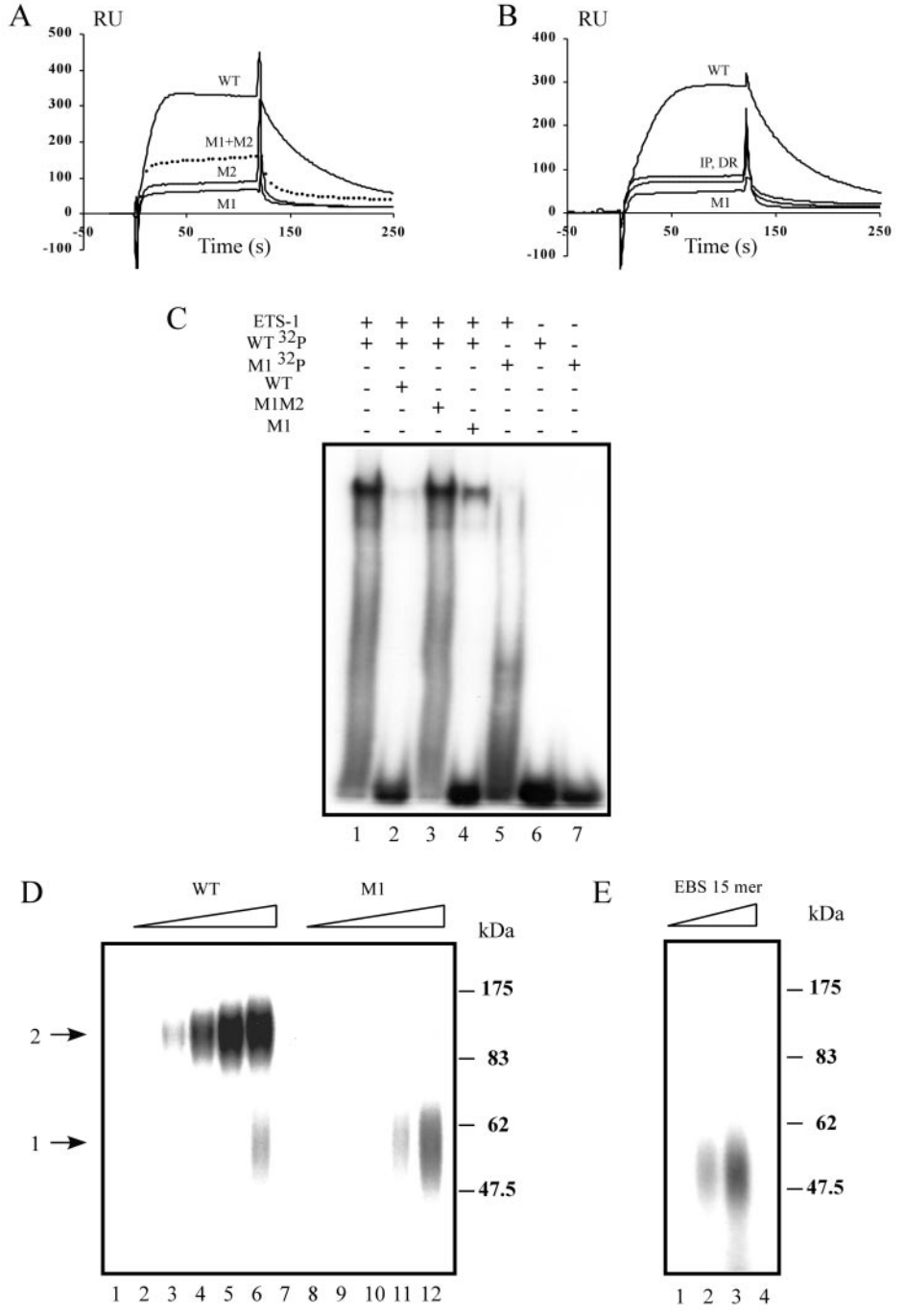

FIG. 1. **ETS-1 specifically binds to the head to head EBS palindrome in a cooperative way.** *A*, sensorgrams of a 200 nM ETS-1 injection over a Sensor Chip functionalized with 280 RU of WT, M1, and M2 oligonucleotides. The *dotted line* represents the sum of M1 and M2 sensorgrams. *B*, sensorgrams of a 200 nM ETS-1 injection over a Sensor Chip functionalized with 260 RU of WT, DR, IP, and M1 oligonucleotides (IP sensorgram comes from another Sensor Chip with the same amount of immobilized DNA). *A* and *B*, a flow cell functionalized with M1M2 oligonucleotides was used as a reference for nonspecific binding. *C*, gel shift assay. ETS-1 (4 pmol) was incubated with WT (*lanes 1–4*) or M1 (*lane 5*) ^{32}P-labeled DNA probe (0.5 ng) in the absence (*lane 1*) or in presence of WT (200×, *lane 2*), M1M2 (200×, *lane 3*), and (M1 400×, *lane 4*) unlabeled competitors, WT (*lane 6*), and M1 (*lane 7*) free probes were loaded. *D*, photo-cross-linking assay resolved by SDS-PAGE. The same amount of ETS-1 (4 pmol) was incubated with increasing amounts (0.125, 0.25, 0.5, 1, and 2 ng) of WT (*lanes 2–6*) or M1 (*lanes 8–12*) ^{32}P-labeled DNA probe prior addition of photo-cross-linker ($Ru(bpy)_3Cl_2$, ammonium persulfate) and illumination. *Lanes 1* and *7* are controls containing 2 ng of WT or M1 probe, respectively, cross-linked in the absence of ETS-1. *E*, same experiment as *D*, realized with an equimolar mixture of ^{32}P-labeled 15-mer oligonucleotides (referred to as 15-mer) corresponding to −223/−209 and −208/−194 sequences of the stromelysin-1 promoter as a probe (0.5, 1, and 2 ng, *lanes 1–3*). *Lane 4* is a control containing 2 ng of probe in absence of ETS-1. The *arrow 1* indicates binary ETS-1·DNA complex. The *arrow 2* indicates ternary ETS-1·DNA·ETS-1 complex.

eration by a 60-s injection of 0.03% SDS in distilled water. Each injection was repeated three times to obtain a complete data set of 12 curves. Raw data were corrected by subtraction of the blank curve corresponding to M1M2 oligonucleotide. Each data set was globally fitted with Biaeval® 3.1 software. The schematic representation of the models that we edited and used for the data analysis and their related set of differential rate equations are listed in Table III. For each model, the kinetic parameters as well as the maximum binding capacity of the immobilized ligand were considered as global parameters for a given data set. Moreover, two local parameters were added for each curve to take into account the refractive index changes at the beginning of the wash-on and wash-off phase.

Transfection and Reporter Gene Assay—HEK293 cells were grown in Dulbecco's modified Eagle's medium supplemented with 10% fetal calf serum in 12-well plates (2 ml per well) to reach 60–80% confluence at the time of transfection. Efficiency of transfection was tested with a β-galactosidase encoding expression vector under the control of the cytomegalovirus promoter after coloration of the transfected cells with 5-bromo-4-chloro-3-indolyl-β-D-galactopyranoside (X-gal) (Roche Molecular Biochemicals). Before transfection, Exgen 500 Transfection Reagent (1.5 μl per well, Euromedex) was incubated with 250 ng of each respective reporter (pGL3) and expression vector (pSG5) for 10 min at room temperature in a volume of 50 μl of a 150 mM NaCl solution. Cell medium was changed for 500 μl of Opti-MEM (Invitrogen), and DNA-Exgen 500 mixture was added. After 16 h, medium was changed for 2 ml of Dulbecco's modified Eagle's medium. Cells were harvested 48 h after transfection with 250 μl of cell lysis buffer (1% Triton X-100, 25 mM glycylglycine, pH 7.8, 15 mM $MgSO_4$, 4 mM EGTA, 1 mM DTT). 20-μl aliquots of each supernatant were tested for luciferase activity (luciferase assay kit, Promega) using a Lumat LB 9501 (Berthold). The expression of the proteins of interest (ETS-1 p51 or p42) was tested by Western blot analysis on total cell lysates using a primary antibody directed against the ETS-1 DBD (C-20, Santa Cruz Biotechnology).

RESULTS

SPR Measurement of the Cooperative Binding of ETS-1 to the EBS Palindrome of the Stromelysin-1 Promoter—To investigate the characteristics of the interaction between ETS-1 and the head to head EBS palindrome located −216/−201 in the stromelysin-1 promoter (referred to as wild type (WT) in the following), several mutants of the EBS repeat were produced. Either one (M1 or M2) or both (M1M2) EBS were inactivated by directed mutagenesis exchanging the 5′-GGAA-3′ core consensus with 5′-AAAA-3′ (Table I). Biotinylated PCR fragments of the −276/−177 region were used as a ligand for SPR measurements of the interaction between ETS-1 and the EBS palindrome (Fig. 1*A*). We observed a positive cooperative binding to the WT site in comparison to M1 or M2 mutants. Indeed, the measured RU signal corresponding to the ETS-1 binding to the WT site was higher than the sum of the RU signal for M1 and M2 mutants (*dotted line* on Fig. 1*A*). To determine whether the cooperative binding was dependent on the mutual orientation of the EBS, we produced mutants in which one (direct repeat, referred to as DR) or both (inverted palindrome, referred to as IP) EBS orientations were changed, taking care to preserve their flanking sequence (Table I). SPR measurements showed a complete disappearance of the cooperative binding to the IP and DR sites as binding to these mutants was approximately twice the binding to the M1 site (Fig. 1*B*).

This quantitatively confirms the observation that ETS-1 or ETS-2 tends to bind head to head EBS palindromes, such as those encountered in GATA-1 (38) or p53 (39) promoters, better than a single EBS or other topology of EBS repeats (44). The fact that ETS-1 could be able to discriminate between different topologies of EBS repetitions tends to prove that this effect could not be driven by structural effects like cooperative bending of the DNA facilitated by the proximity of the EBS. Indeed structural studies showed that ETS DNA binding domain (DBD) binding to DNA induces moderate bending (45, 46). If such a phenomenon was the unique strength of the cooperativity, binding to IP and DR mutant sites would also be enhanced by the DNA bending generated by the first ETS-1 molecule. Then other mechanisms, like protein-protein interactions, should be envisaged.

Visualization of ETS-1-DNA Complexes by EMSA and Photo-cross-linking—The major drawback of BIAcore® technology is its inability to identify the complexes formed between the ligand and the analyte during the injection time. So we confirmed our observations by visualizing the protein-DNA complexes at the equilibrium by EMSA and photo-cross-linking.

EMSA showed the formation of a single major complex between ETS-1 and the WT probe (Fig. 1*C*, *lane 1*). Whereas a 200× molar excess of WT non-labeled probe was able to disrupt this complex (Fig. 1*C*, *lane 2*), a 400× molar excess of M1 probe, corresponding to the same amount of binding sites, was unable to do so (Fig. 1*C*, *lane 4*). Moreover, the association of ETS-1 with M1 probe only led to a weak fading signal (Fig. 1*C*, *lane 5*) in comparison to the WT complex, and thus with the same protein and probe amounts (compare *lanes 1* and *5* on Fig. 1*C*). Similar results were obtained with M2 probe (data not shown). This experiment confirms the cooperative binding of ETS-1 to the head to head EBS palindrome present in the stromelysin-1 promoter.

In order to visualize the complex formed with M1 probe, which did not seem to resist migration through the polyacrylamide gel used under our experimental conditions, we performed cross-linking with $Ru(bpy)_3Cl_2$. This reagent enabled instant high yield cross-linking with no bridging agent (47). At low probe concentrations, only a weak signal was visible with WT probe (Fig. 1*D*, *lane 3*), and no signal was observed with M1 (Fig. 1*D*, *lanes 8–10*). This signal, migrating at ~120 kDa, corresponds to two ETS-1 molecules linked to the WT probe. Increasing the probe concentration results for the M1 probe (Fig. 1*D*, *lanes 11* and *12*) in the formation of a weak complex at about 60 kDa corresponded to a single ETS-1 molecule linked to the probe. This signal appeared as the concentration of WT probe increased (Fig. 1*D*, *lane 6*) but remained less intense than the 120-kDa signal. Interestingly, no signal was observed at 120 kDa in an experience using an equimolar mixture of ^{32}P-labeled oligonucleotides corresponding to −223/−209 and −208/−194 sequences of the stromelysin-1 promoter as a probe (referred to as EBS 15-mer in Fig. 1*E*). We obtained a pattern similar to M1, although we could have hoped to restore a trimeric complex by protein-protein interactions. This suggests that if such contacts exist, they are dependent on the strict vicinity and positioning provided by the topology of the palindromic binding sites.

Kinetic Study of the Interaction between ETS-1 and the Stromelysin-1 Promoter—We characterized the binding cooperativity by modeling the interaction between ETS-1 and the EBS palindrome of the stromelysin-1 promoter. New data sets were produced under conditions more favorable for kinetic studies as follows: (i) lower binding capacity (100 RU of immobilized DNA) and higher flow rate (30 μl/min) to reduce mass transfer effects at the surface of the Sensor Chip; (ii) lower temperature to reduce kinetic rates; and (iii) addition of bovine serum albumin to 100 μg/ml in the running buffer to prevent excessive refractive index changes during injections. A typical quadruplet of curves for each oligonucleotide (M1, M2, and WT) is shown in Fig. 2. The kinetic models used to fit the data sets and the related differential rate equations are represented in Table III. Kinetic and equilibrium parameters obtained for each model are listed in Table IV.

ETS-1 binding to M1 or M2 oligonucleotides was fitted according to the simplest kinetic model provided, a one to one interaction. ETS-1 binding to the WT oligonucleotide was fitted with our own edited models of increasing complexity, representing the possible interactions of two ETS-1 molecules with DNA. We tried to keep to a minimum the number of kinetic parameters in order to preserve the significance of the model. We considered models in which binding of the two ETS-1 molecules could be independent (models A and B) or sequential (models C and D). We also introduced the possibility of a conformational change of the ternary complex after binding to the DNA (models B and D). In addition to the kinetic parameters, for each of these models we calculated in Table IV an apparent binding affinity corresponding to the affinity of two independent and equivalent EBS, referred to as $K_{d(app)}$, giving

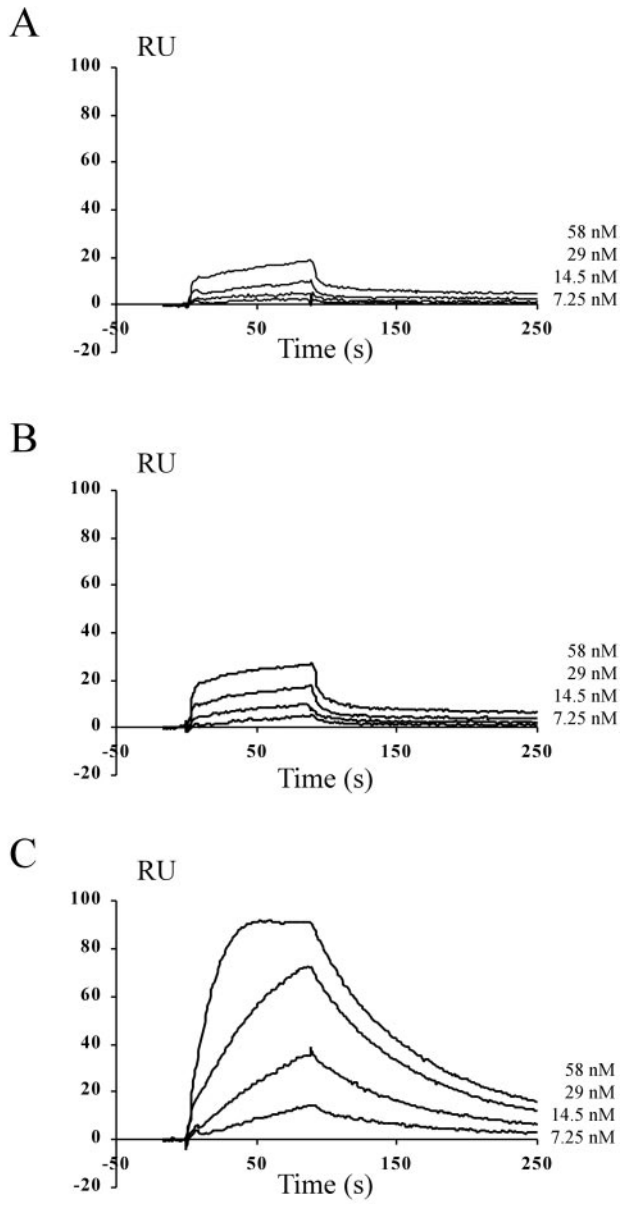

FIG. 2. **Surface plasmon resonance kinetic analysis of ETS-1 interaction with the EBS palindrome of the stromelysin-1 promoter.** Representative set of sensorgrams illustrating the real time binding of various concentrations (7.25, 14.5, 29, and 58 nM) of ETS-1 to the M1 (*A*), M2 (*B*), and WT (*C*) stromelysin-1 promoter. M1M2 mutant was used as a reference for nonspecific binding. Analysis was performed as described under "Materials and Methods." Kinetic models used and results are summarized in Tables III and IV, respectively.

the same global affinity. This apparent affinity enabled us to determine, in each case, the binding cooperativity in comparison to the M1 and M2 oligonucleotides (see Table IV for results and equations).

The fitting data show that, in the presence of two binding sites, kinetics seem to be faster (compare k_{a1} and k_{d1} with M1 or M2 and the WT models in general) but without considerably altering the overall equilibrium constants (compare K_{d1} values). This can be due to a difference of accessibility to the DNA or more likely to the difference in binding mechanisms between both DNA configurations (M1 or M2 in comparison to WT). Considering the χ^2 values of the models, it is obvious that simple model depicting independent binding sites (model A) is insufficient to describe the overall binding mechanism. Nevertheless, adding a conformational change after DNA binding (model B) improves fitting (χ^2 from 3.4 to 2.77). In that case, K_d values (K_{d1} and K_{d2}) are similar to the K_{d1} values obtained for M1 and M2, and the conformational change provides the 6.7-fold cooperativity for the ternary complex formation.

In order to describe better a cooperative mechanism, a sequential binding (models C and D), where the binding of the first molecule is able to influence the binding of the second one, seems to be more accurate. Evidence of this is the fact that the calculated cooperativity fold increases according to the χ^2 value. A simple sequential model (model C) provides a better χ^2 value than model A (2.65 compared with 3.4), which uses the same number of parameters but with independent binding sites. It is noteworthy that K_{d1} between model A and C is not greatly affected, but K_{d2} is 3-fold lower, in accordance with the definition of a cooperative binding mechanism. Indeed the reduction of K_{d2} is mainly due to an increase of k_{a2}, reflecting a better association of the second protein to the complex. The last model (model D), comprising a sequential binding followed by a conformational change, provides the better χ^2 of the series (0.996) and so the best description of the cooperative phenomenon. As for model C, but to a greater extent, the K_d value of the second step (K_{d2}) is reduced compared with the first one (about 50 times lower than K_{d1}) or to the second step of model B (about 20 times lower) which uses the same number of parameters but with independent binding sites. In both cases this reduction is due to the increase in k_{a1} values. The K_{d3} value of 0.95 indicates that at the equilibrium the ternary complex exchanges freely between two conformations. The cooperativity fold is then maximum for this model reaching 19.7-fold for a $K_{d(app)}$ of 18.7 nM.

This kinetic study confirms the cooperative binding of two ETS-1 molecules to the EBS palindrome. The cooperativity observed seems to be driven by the facilitated binding of the second ETS-1 molecule to form the ternary complex rather than by the formation of a ternary complex in a locked conformation after a conformational change as k_{d2}, k_{a3}, and k_{d3} gave no evidence of it. Indeed, in that case we would have encountered slower dissociation steps for the ternary complex, with lower k_{d2} and k_{d3} values.

Mapping of the Protein Region Responsible for the Cooperative Binding by N-terminal Deletion Mutants of ETS-1 Protein—In order to determine whether a particular protein region was responsible for the observed cooperative behavior, we produced N-terminal deletion mutants of ETS-1 by PCR amplification and cloning into pTyb2 vector for bacterial expression (Fig. 3*A*). Recombinant proteins were purified as under "Materials and Methods." A SDS-PAGE of the various mutants was silver-stained to assess purity (Fig. 3*C*).

The ability of the different deletion mutants to cooperate for binding to the EBS palindrome was evaluated by SPR measurement at the equilibrium (Fig. 4*A*). The same concentration (200 nM) of each protein was injected over a Sensor Chip functionalized with WT, M1, and M2 oligonucleotides. At the end of the injection, when binding equilibrium was reached, and after blank correction using M1M2 oligonucleotide, RU signal for each flow cell was measured, and the following ratio was calculated: WT/M1 = RU(WT)/RU(M1). Results are displayed in Fig. 4*B*. The WT/M2 and WT/(M1 + M2) ratios, also representative of the cooperative binding of the proteins to DNA, showed similar variations (data not shown) and so will not be mentioned in this study. We observed a rapid increase of the WT/M1 ratio from ΔN331, which represents a DBD without its N-terminal inhibitory region, to ΔN245. For deletion mutants beyond amino acid 245, it stabilized at a value corresponding to the ratio obtained with the full-length protein.

RU variation is representative of a mass variation at the surface of the Sensor Chip with the correlation that 1000 RU

TABLE IV

Kinetic and equilibrium parameters for ETS-1 interaction with the EBS palindrome of the stromelysin-1 promoter, as determined by surface plasmon resonance.

All the notations for the parameters are consistent with the ones used in Table III.

Ligand	k_{a1}	k_{d1}	K_{d1}[a]	k_{a2}	k_{d2}	K_{d2}[a]	k_{a3}	k_{d3}	K_{d3}[a]	$K_{d(app)}$[a,b]	Cooperativity fold (α)[b,c]	χ^2
	$(x10^6)\ M^{-1}\ s^{-1}$	$(x10^{-3})\ s^{-1}$	*nM*	$(x10^4)\ M^{-1}\ s^{-1}$	$(x10^{-3})\ s^{-1}$	*nM*	$(x10^{-3})\ s^{-1}$	$(x10^{-3})\ s^{-1}$		*nM*		
M1	2.00 ± 0.02	2.10 ± 0.04	105 ± 2									0.255
M2	2.90 ± 0.02	1.90 ± 0.01	65.5 ± 0.6									0.507
WT, model A	32.0 ± 0.8	20.1 ± 0.1	62.8 ± 1.6	10.9 ± 1.0	5.90 ± 0.3	54.1 ± 5.7				58 ± 3	2.02 ± 0.22	3.4
WT, model B	18.9 ± 1.7	20.4 ± 1.6	108 ± 13	24.9 ± 1.8	14.8 ± 0.5	59.7 ± 4.7	2800 ± 400	450 ± 60	0.16 ± 0.03	32 ± 4	6.7 ± 1.6	2.77
WT, model C	46.0 ± 0.7	20.0 ± 0.1	43.5 ± 0.7	36 ± 1	6.5 ± 0.1	18.1 ± 0.6				28.0 ± 0.5	8.80 ± 0.4	2.65
WT, model D	27.0 ± 0.1	36.0 ± 0.7	133 ± 3	1300 ± 20	36 ± 1	2.80 ± 0.9	7.3 ± 0.2	6.9 ± 0.1	0.95 ± 0.03	18.7 ± 0.5	19.7 ± 1.1	0.996

[a] Incertitude is calculated using the equation:

$$(\Delta y)^2 = \sum_{i=1}^{n} \left(\frac{\partial y}{\partial x_i}\right)^2 (\Delta x_i)^2.$$

[b] Apparent binding affinity of a single EBS of the WT palindrome considered as the juxtaposition of two independent and equivalent binding sites (same K_d and no cooperativity) calculated using the equation:

$$K_{d.app} = \sqrt{\prod_{i=1}^{n} K_{di}}.$$

[c] Cooperativity fold observed between the two EBS of the WT palindrome calculated using the equation

$$\alpha = \frac{K_{d1}^{M1} \cdot K_{d1}^{M2}}{(K_{d.app}^{WT})^2} = \frac{K_{d1}^{M1} \cdot K_{d1}^{M2}}{\prod_{i=1}^{n} K_{di}^{WT}}$$

FIG. 3. **Organization of ETS-1 and its N-terminal deletion mutants.** *A*, map of ETS-1 and its deletion mutants produced with T7 Impact System. *B*, secondary structure of the ETS-1 DBD (α-helices H1-H3 and β-sheets S1-S4) and inhibitory regions (HI-1, HI-2, and H4). *C*, 15% acrylamide SDS-PAGE of ETS-1 and its various deletion mutants, silver-stained according to Ref. 59.

correspond to a variation of 1 ng/mm^2 at the surface. Thus, we were able to estimate the quantity of protein bound per surface unit at the equilibrium for each oligonucleotide (Fig. 4*C*). The binding pattern of the M1 oligonucleotide was consistent with the known mechanism of binding regulation of ETS-1 by autoinhibition (21). Indeed, the amount of protein bound decreased from ΔN301 to ΔN245, as long as the inhibitory module was restored to the protein. But at the same time, despite the complete inhibitory module restoration, the quantity of bound protein to WT oligonucleotide increased and was maximum for ΔN245, resulting in the observed cooperativity. Beyond amino acid 245, the quantity of bound protein to M1 oligonucleotide remained low, and at the opposite end, the quantity of bound protein to WT oligonucleotide was still high but lower than for ΔN245 (this could be due to the presence of the N-terminal part of the protein that may influence DNA binding by sterical or more complex mechanisms). Nevertheless, WT/M1 ratio remains constant from ΔN245 to the full-length protein.

To confirm these results and have evidence of the molecular species involved, we performed EMSA with the different mutants using WT and M1 probes (Fig. 4*D*). We observed the complete reversion of the binding pattern from ΔN331 to ΔN245 (Fig. 4*D*, *lanes 1–8*). ΔN331 forms the same strong binary complex with one protein molecule bound to the probe with M1 or WT oligonucleotides (*lanes 1* and *2*), whereas the ternary complex is hardly visible with the WT probe (Fig. 4*D*, *lane 2*). This remains consistent with the SPR results where the WT/M1 ratio was close to 1 suggesting that at equilibrium a ternary complex was not present with the WT oligonucleotide. ΔN301 was also able to form a binary complex with the M1 probe (Fig. 4*D*, *lane 3*) but also a strong slower migrating

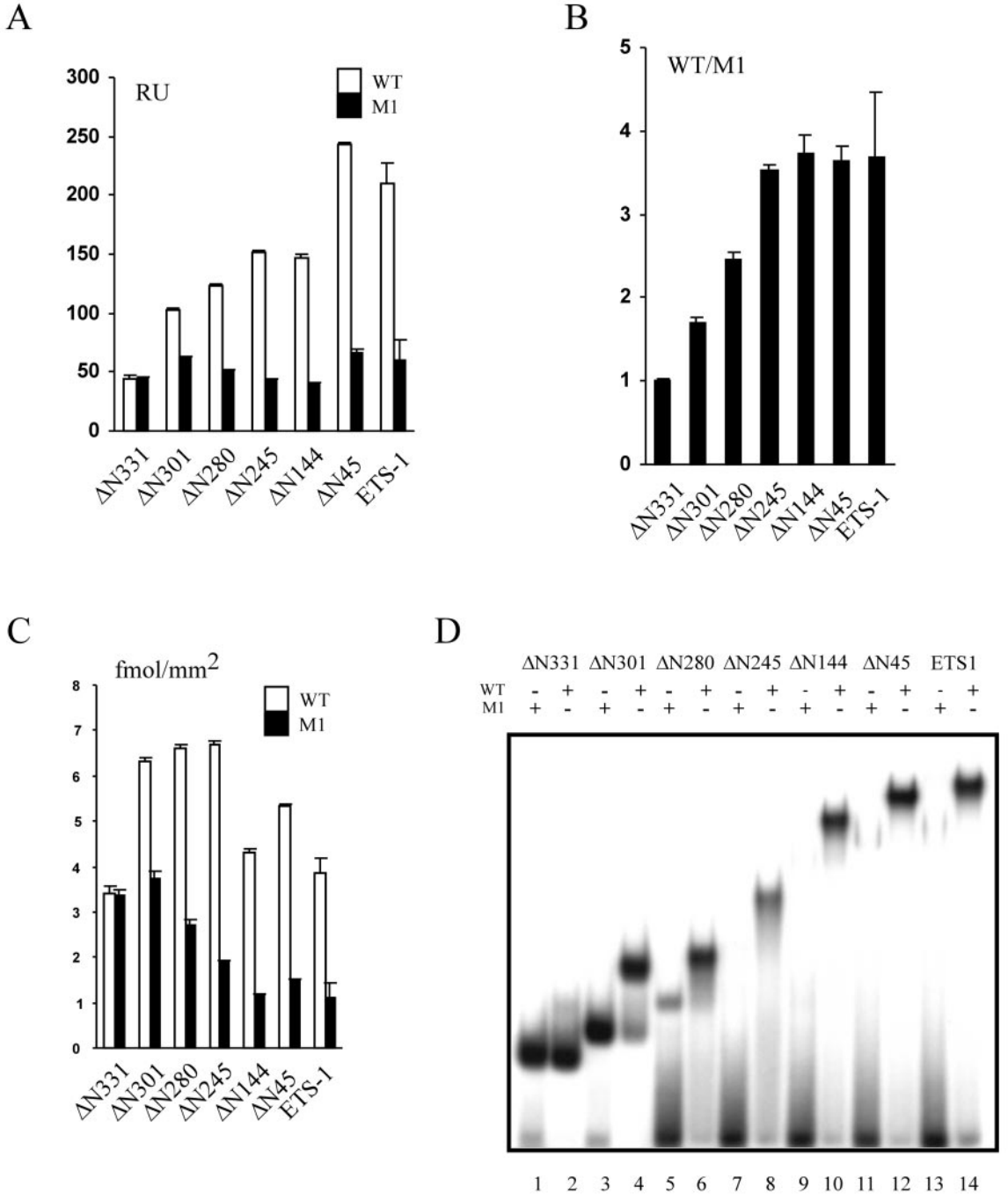

FIG. 4. **Localization of the ETS-1 peptidic region implicated in the stromelysin-1 promoter binding cooperativity.** As for Fig. 1 and Fig. 2, M1M2 oligonucleotide was used as a reference for nonspecific DNA binding. *A*, amount of protein bound to WT and M1 oligonucleotides at the equilibrium phase during a 200 nM injection of ETS-1 or its N-terminal deletion mutants, expressed in RU. *B*, representation of the ratio between the different proteins bound to WT oligonucleotide and M1 oligonucleotide for a 200 nM protein injection. RU for calculation were measured at the end of the injection at equilibrium phase. *C*, protein binding to WT and M1 oligonucleotides, expressed in fmol/mm^2. *D*, gel shift assay. Same amount of ETS-1 or its N-terminal deletion mutants (4 pmol) was incubated with the WT or M1 ^{32}P-labeled probe (0.5 ng).

ternary complex made of two proteins bound to the WT probe (*lane 4*). The binary complex, which was observed with M1, was also present with the WT probe but weaker. ΔN280 binds weakly to the M1 probe (Fig. 4*D*, *lane 5*) and only formed with the WT probe a slower migrating ternary complex (*lane 6*). Binding patterns for ΔN245, ΔN144, ΔN45, and ETS-1 were identical, *e.g.* no distinct complex formed with M1 probe (Fig. 4*D*, *lanes 7*, *9*, *11*, and *13*) and only a strong slower migrating ternary complex formed with WT probe (*lanes 8*, *10*, *12*, and *14*).

These observations tend to designate the region located between amino acid 245 and 331 as responsible for the cooperative binding of two ETS-1 molecules to the EBS palindrome. The mechanism implied is the suppression of the DNA-binding autoinhibition. It seems possible that two ETS-1 molecules overcome DNA binding autoinhibition by a protein-protein interaction in the 245–331-residue region or another mechanism implying this region, during the ternary complex formation, that would favor an unrepressed form with an HI-1 inhibitory helix unwound (see Fig. 3*B* for schematic representation of the structural elements of the ETS-1 DBD and inhibitory regions). Such mechanism has already been described for ETS-1, which

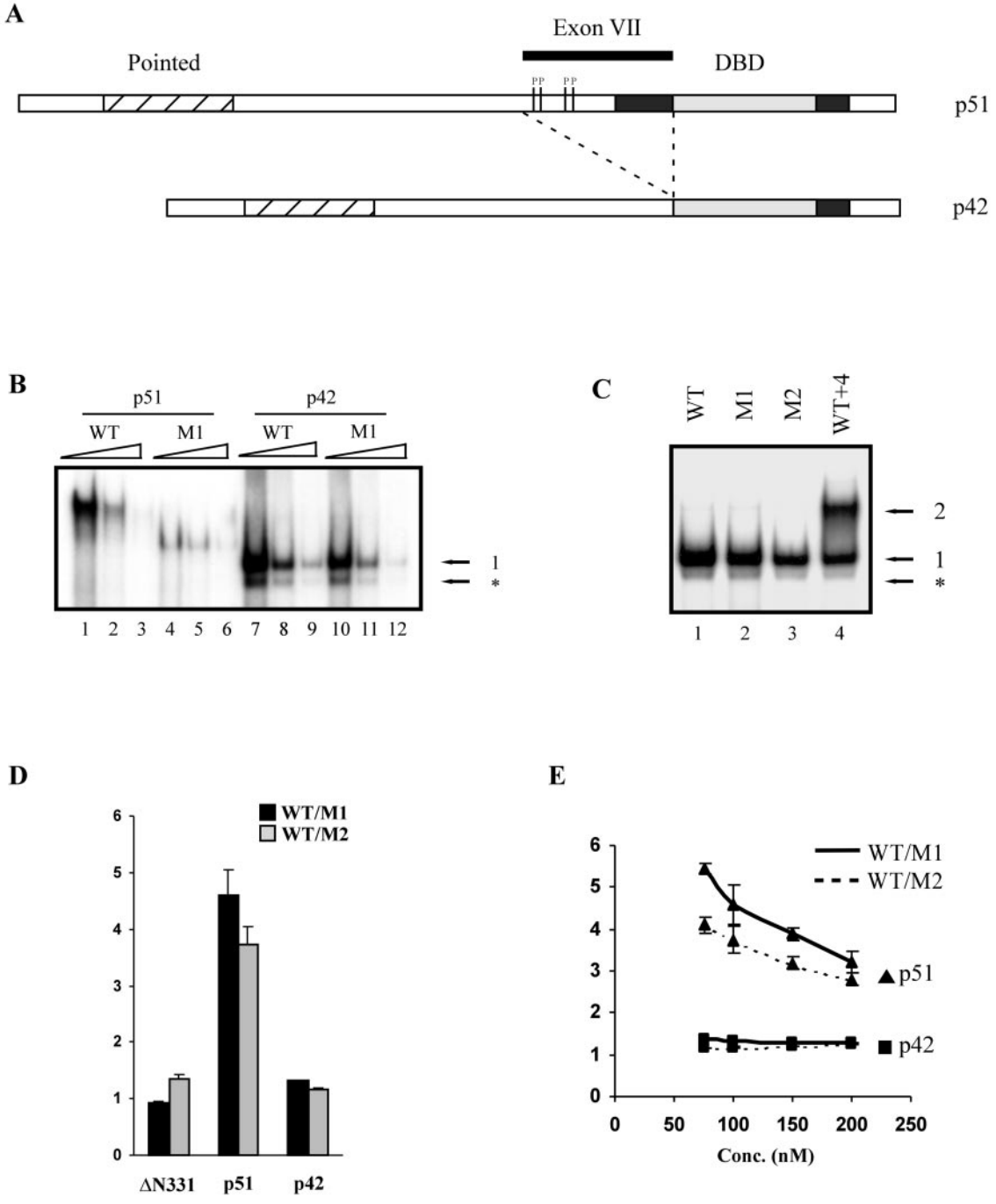

FIG. 5. **Comparison between binding of ETS-1 p51 and p42 isoforms to the EBS palindrome of the stromelysin-1 promoter.** *A*, schematic organization of p51 and p42 isoforms of ETS-1. *P* represents a serine susceptible to be phosphorylated by CaMKII. *B*, gel shift assay. Equal amounts (4 pmol) of ETS-1 p51 (*lanes 1–6*) and ETS-1 p42 (*lanes 7–12*) isoforms are incubated with WT (*lanes 1–3* and *7–9*) or M1 (*lanes 4–6* and *10–12*) ^{32}P-labeled oligonucleotides (0.5 ng) in the presence of increasing amounts of unlabeled competitor (50× *lanes 2*, *5*, *8*, and *11*, and 200× *lanes 3*, *6*, *9*, and *12*). *C*, gel shift assay. The same amount (4 pmol) of ETS-1 p42 was incubated with WT (*lane 1*), M1 (*lane 2*), M2 (*lane 3*), and WT + 4 (*lane 4*) ^{32}P-labeled probes (0.5 ng). *D*, SPR experiment. Ratio of protein bound to WT and M1 or WT and M2 oligonucleotides during the equilibrium phase of a 100 nM p51 or p42 injection. *E*, variation of the previous ratios as a function of the analyte (▲, p51, or ■, p42) concentration (75, 100, 150, and 200 nM). The *arrow 1* corresponds to the binary p42·DNA complex, and *arrow 2* to the ternary p42·DNA·p42 complex, and the *arrow* * to a complex formed with a minor contaminant.

was able to interact with a binding partner in order to stabilize its unrepressed conformation (29, 31). It would account for the easier and faster formation of the ternary complex emphasized by the kinetic study.

Binding Pattern of the p42 Isoform of ETS-1 to the EBS Palindrome of the Stromelysin-1 Promoter—ETS-1 physiologically exists under two different isoforms: p51, the full-length protein, and p42, a shorter isoform that lacks the 245–331-residue region encoded by exon VII of the gene (Fig. 5*A*). These two proteins, although sharing similar characteristics due to their common DBD and pointed domain, also have distinct properties (48, 49). It was particularly interesting to study the binding of the ETS-1 p42 isoform to the EBS palindrome of the stromelysin-1 promoter. Its cDNA was cloned in a pTyb2 vector and the recombinant protein was expressed and purified (see "Material and Methods").

By using EMSA, we compared DNA binding to WT and M1 probes for the ETS-1 p51 and p42 isoforms. Surprisingly, p42

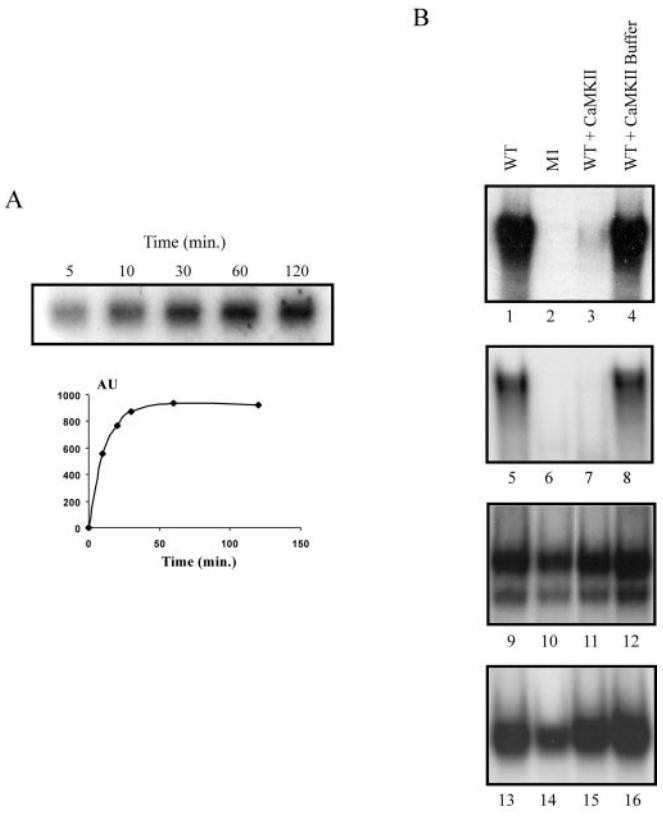

FIG. 6. **Effect of ETS-1 phosphorylation by CaMKII on the cooperative binding to the head to head EBS palindrome of the stromelysin-1 promoter.** *A*, phosphorylation kinetics of ETS-1 p51 by recombinant rat CaMKII in the presence of [γ-^{32}P]ATP. *AU*, arbitrary units. *B*, gel shift assay. Equal amounts (4 pmol) of ETS-1 p51 isoform (*lanes 1–4*), ΔN245 (*lanes 5–8*), ETS-1 p42 isoform (*lanes 9–12*), and ΔN331 (*lanes 13–16*) were incubated with WT ^{32}P-labeled oligonucleotides (0.5 ng, all *lanes* except *2*, *6*, *10*, and *14*), M1 ^{32}P-labeled oligonucleotide (0.5 ng, *lanes 2*, *6*, *10*, and *14*) after phosphorylation by CaMKII (*lanes 3*, *7*, *11*, and *15*), or after incubation with phosphorylation buffer without kinase (*lanes 4*, *8*, *12*, and *16*).

showed no binding difference between WT and M1 oligonucleotides (Fig. 5*B*, *lanes 7* and *10*). Because only one EBS is present within M1 probe and no ETS-1-ETS-1 interaction is reported in the literature, this suggests that only a binary complex formed with both probes. The minor faster migrating band observed (Fig. 5*B*, *arrow* *, *lanes 7* and *10*, and also Fig. 6*B*) could be due to a minor contaminant present in the p42 protein preparation and cannot be considered as the binary complex, whereas the upper band would be the ternary complex. Indeed, both complexes were observed with the two probes, whereas M1 cannot bind more than one ETS-1 molecule (Fig. 1*D*) because only one EBS is present. Moreover, increasing the spacing between both EBS of 4 bp (see WT + 4 in Table I) results in the formation of a slower migrating complex corresponding to the expected ternary complex (Fig. 5*C*, *lane 4*), whereas only a binary complex is observed with WT, M1, and M2 probes (Fig. 5*C*, *lanes 1–3*). Finally, the formation of the same complex with M1 and WT probes was previously encountered with ΔN331 (Fig. 4*D*), which also lacks the 245–331-residue region. It reinforces the crucial role of this region for ETS-1 ability to discriminate the EBS topology on DNA.

The same SPR equilibrium measurements as for the ETS-1 deletion mutants were carried out with ETS-1 p42 isoform on WT, M1, and M2 oligonucleotides (Fig. 5*D*). The WT/M1 and WT/M2 ratios calculated for p42 isoform are close to that of ΔN331, the shortest deletion mutant lacking the 245–331-residue region, reflecting the loss of cooperativity and its inability to form a ternary complex with the WT oligonucleotide. The influence of protein concentration on the cooperative binding mechanism was evaluated by measuring the previous ratios for different concentrations (Fig. 5*E*). Their variation for p51, increasing for low concentrations where the cooperative factor is high, is in agreement with a cooperative behavior. On the contrary, for p42 isoform, the near 1 ratio value is independent on the protein concentration. All together, these data demonstrate the implication of the 245–331-residue region encoded by exon VII in the human ETS-1 cooperative binding to the head to head EBS palindrome present in the stromelysin-1 promoter.

Effects of ETS-1 Phosphorylation by CaMKII on Cooperative Binding to the EBS Palindrome of the Stromelysin-1 Promoter—Calcium-dependent phosphorylation of ETS-1 on residues Ser-251, Ser-257, Ser-282, and Ser-285 was reported to negatively regulate ETS-1 DNA binding *in vitro* and *in vivo* (50, 51). The proposed mechanism is a reinforced autoinhibition by stabilization of the inhibitory conformation through electrostatic interactions between phosphoserines and basic residues of the inhibitory module.

In order to extend our model and to determine the influence of calcium-dependent phosphorylation on the ETS-1 cooperative binding, we realized *in vitro* phosphorylation assays using CaMKII. First, we realized phosphorylation kinetics using ETS-1 as a substrate to determine time conditions under which phosphorylation was maximum for the amount of substrate and enzyme considered (Fig. 6*A*). We further used a 90-min incubation corresponding to the stationary phase of the reaction.

Phosphorylation effects were tested by EMSA, comparing binding to the WT probe of ETS-1 p51 and p42 isoforms incubated in the presence or absence of CaMKII. We also tested phosphorylation effects on ΔN331, which lacks calcium-dependent phosphorylation sites, and ΔN245, which both have a similar binding behavior to p42 and p51, respectively. For ETS-1 p51 isoform and ΔN245, hardly any binding of the phosphorylated proteins was observed with the WT probe (Fig. 6*B*, *lanes 3* and *7*). For ΔN331 or ETS-1 p42 isoform no significant difference in amounts of bound protein between the CaMKII-treated sample and the control (Fig. 6*B*, *lanes 11* and *15*) was observed. These results confirm the role of autoinhibition and the implication of the 245–331-residue region in the cooperative binding to the EBS palindrome. It seems that reinforcing autoinhibition by phosphorylation of the serine residues reduces dramatically the cooperative binding. This can be explained either by the stabilization of the inhibitory conformation of ETS-1, which reduces affinity for DNA, or by a possible electrostatic repulsion of the negatively charged phosphoserines that would prevent protein-protein interaction in the 245–331-residue region.

Activation of the Stromelysin-1 Promoter by ETS-1 p51 and p42 Isoforms—It was interesting to investigate whether the difference of DNA binding of the p51 and p42 isoforms was correlated with their transcriptional activation. The −478/+4 region of the WT, M1, M2, and M1M2 stromelysin-1 promoters was cloned in the pGL3 basic vector (Fig. 7*A*). These vectors were co-transfected with either p51 or p42 eukaryotic expression vectors in HEK293 cells. Culture lysates were tested for luciferase activity. For p51, mutation of one of both EBS sites had dramatic effect on transactivation, resulting in an ~90% loss of activity. Double mutation readily abolished activation by p51. These results, obtained with ETS-1, were similar to those obtained with ETS-2 protein on the human stromelysin-1 promoter (13). This experiment provides a direct link between cooperative DNA binding and functional transactivation. Interestingly, the ETS-1 p42 isoform did not activate the stromely-

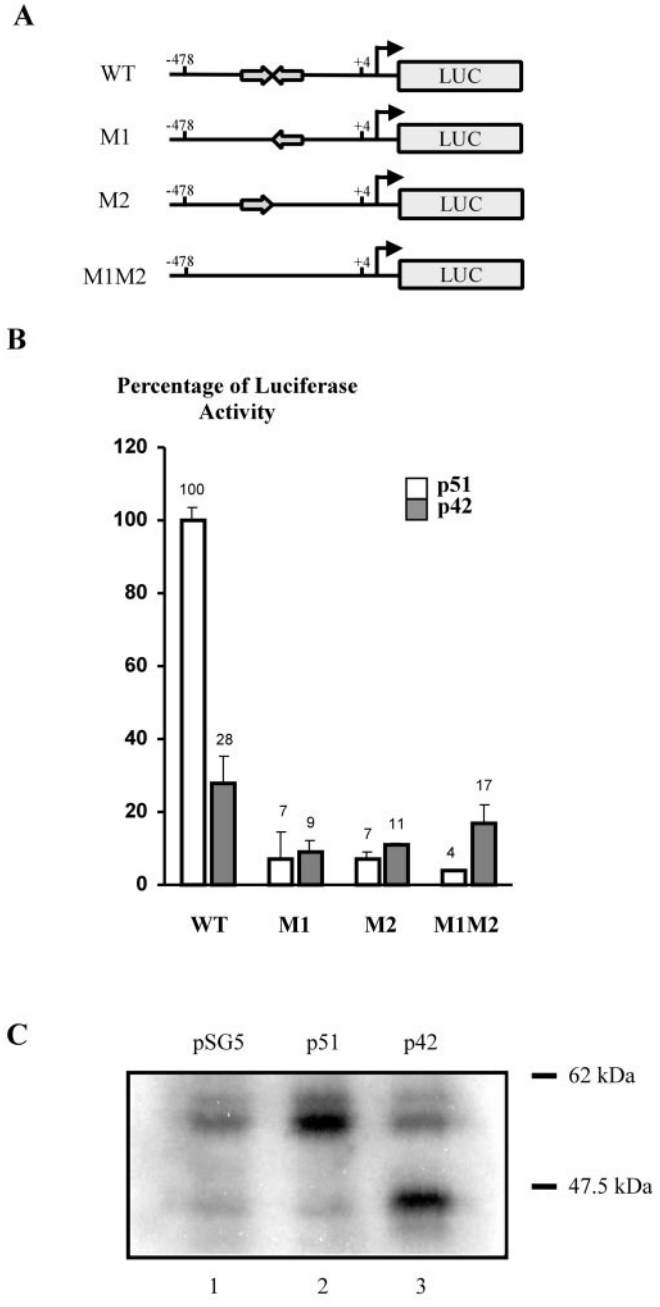

FIG. 7. **Activation of the stromelysin-1 promoter by ETS-1 p51 and p42 isoforms.** *A*, reporter gene constructs used for the transient transactivation assay. The −478/+4 region of the WT and mutant stromelysin-1 promoters was cloned into a pGL3basic vector, and *LUC* represents the luciferase reporter gene. *B*, transient transfection assays are realized using HEK293 cells at 60–80% confluence. 250 ng of each luciferase reporter vector were co-transfected with 250 ng of either p51 or p42 eukaryotic expression vector. Luciferase activities obtained were expressed as a percentage of the WT promoter activity co-transfected with the p51 expression vector (3.9-fold). Exact percentages are indicated on *top* of the *bars.* Results are the average of two representative experiments done in triplicate. *C*, Western blot analysis of HEK293 cell lysates after transfection with pSG5 (*lane 1*), pSG5-p51 (*lane 2*), and pSG5-p42 (*lane 3*). The primary antibody used is directed against ETS-1 DNA binding domain (C-20, Santa Cruz Biotechnology).

sin-1 promoter in the same way as the p51 isoform did (only 28%). Western blot analysis of the ETS-1 proteins in cell lysates after transfection (Fig. 7*C*) showed no significant difference between p51 and p42 expression. Thus, differential expression of the proteins cannot be responsible for the observed difference in transactivation. We can infer that either p42 does not share the same transcriptional activity as p51 or that the presence of two ETS-1 molecules and their proper spatial orientation are required for maximum activation of the stromelysin-1 promoter.

DISCUSSION

The human stromelysin-1 promoter has been shown to be differently regulated by various members of the ETS family through the EBS palindrome located −216/−201. ETS-1, ETS-2 (13, 14), and PEA-3 (52) are transcriptional activators, whereas TEL is reported to repress the gene (53). In addition, ETS-related gene (ERG) is able to inhibit the transcriptional activation mediated by ETS-2 (40). In this study, we investigated the mechanism of ETS-1 binding to this palindrome. We confirmed that DNA binding is cooperative, requiring the head to head orientation of the EBS and their strict vicinity (Fig. 1), which is fully consistent with results obtained with other EBS palindromes (39, 44). An anterior report showed cooperative transactivation, whereas no cooperative binding to the EBS palindrome was observed (14). By working with purified proteins and a homologous system, we showed cooperative binding with no ambiguity in comparison to this former study realized in a heterologous system. Kinetic analysis of ETS-1 binding to the WT promoter (Fig. 2 and Tables III and IV) confirms this hypothesis and enables us to give a plausible mechanism for the cooperativity. The binary complex formed between one ETS-1 molecule and an EBS facilitates the fast binding of the second ETS-1 molecule to form the ternary complex. The high rate of this step could be explained by a protein-protein contact between ETS-1 molecules that would give the right orientation, positioning, and conformation for the second ETS-1 molecule to recognize the EBS. By using deletion analysis of the ETS-1 protein, we further demonstrated that the 245–331-residue region, encoded by exon VII of the gene, was responsible for the observed cooperativity (Figs. 3 and 4), and this strongly suggests that the alleviation of the DNA binding autoinhibition is implicated in the cooperative binding. The sum of the kinetic and equilibrium SPR analyses causes us to propose the following binding model (Fig. 8) in which the first ETS-1 molecule bound to DNA facilitates the binding of a second ETS-1 molecule through an interaction implying the exon VII-encoded region. The second ETS-1 molecule would be presented in the right orientation and in an uninhibited conformation, explaining the binding cooperativity observed. This molecular event is represented in Fig. 8 with *square brackets*. The ETS-1 molecules contact through their exon VII-encoded region, and the DNA-bound ETS-1 molecule helps the second one to acquire its open uninhibited conformation in the right orientation to bind DNA, according to the palindromic topology of the binding sites. After formation of the ternary complex, the ETS-1 molecules flip between two conformations on DNA corresponding to the last equilibrium of the figure. According to the model, we proposed it to be a conformational change between the exon VII-encoded regions which were implicated in the previous step of the mechanism and could then adopt a relaxed conformation after the ternary complex was formed.

This may have biological significance because the natural ETS-1 p42 isoform, lacking the exon VII-encoded region, fails to bind cooperatively to the EBS palindrome and allows the binding of only one p42 molecule (Fig. 5). The absence of the inhibitory helices HI-1 and HI-2, preventing the formation of the postulated compact inhibitory bundle, could generate sterical hindrance and account for this result (see Figs. 3, *A* and *B*, and 5*A* and Ref. 21 for structural elements of ETS-1). This phenomenon was also encountered with the shorter ΔN331 deletion mutant. Therefore, the C-terminal region of p42 or ΔN331, spanning amino acids 416–441 and comprising the H4 inhibi-

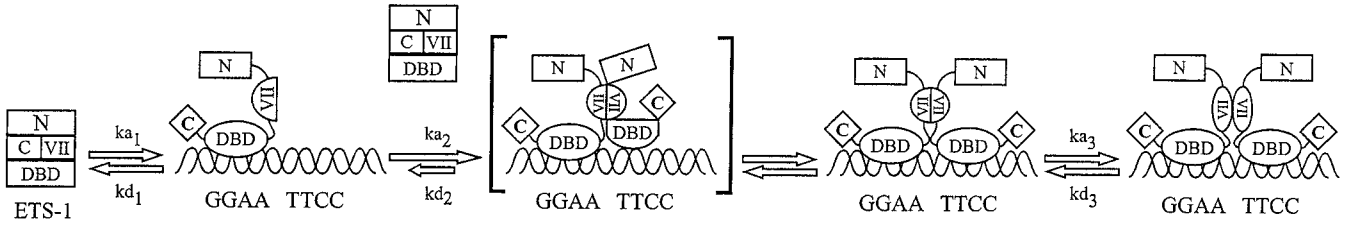

FIG. 8. **Proposed model for ETS-1 cooperative binding to the stromelysin-1 promoter.** It was based on kinetic and equilibrium analyses of ETS-1 interaction with the EBS palindrome of the stromelysin-1 promoter and on ETS-1 known structure and binding mechanism. *N* and *C* represent the N-terminal and C-terminal part of ETS-1, respectively. We propose that after binding to DNA (first step corresponding to k_{a1} and k_{d1} parameters), the first ETS-1 molecule facilitates the binding of the second one by positioning and helping it to reach its uninhibited state through a contact involving the exon VII-encoded region (second step corresponding to k_{a2} and k_{d2}). The intermediary state where the first ETS-1 molecule contacts the second one before the complete formation of the ternary complex is represented by *square brackets*. After formation of the ternary complex, ETS-1 molecules are able to adopt a relaxed conformational state (last step corresponding to k_{a3} and k_{d3}). We propose it to be a conformational change between the exon VII-encoded regions that were implicated in the previous step and could rearrange once the ternary complex is formed.

tory helix, could be responsible for the observed binding inhibition of a second p42 or ΔN331 molecule to the DNA because, except for the DBD, it is the only region they share in common. Such a mechanism remains hypothetical because recent co-crystallization of ETS-1 amino acids 331–440 with Pax5 (54) shows no evidence of a C-terminal region (comprising H4) extending away from the DBD. Other possibilities could be envisaged independently or in conjunction. Indeed, differential DNA bending between p51 and p42, which we rejected to explain the binding cooperativity of p51 because it was dependent on the EBS orientation, could contribute in this case to prevent a second p42 molecule from entering into the major groove of the DNA. A way to link destructuring of the inhibitory module with the differential DNA bending is the recently elucidated mechanism of interaction between the N-terminal end of helix H1 and the phosphate backbone of the DNA (55). A difference of H1 conformation between p42 and p51, linked to the absence of an inhibitory module, would influence DNA bending through a different neutralization of the phosphate backbone charge by H1.

Our results appear of interest in the context of the complex regulation of stromelysin-1 expression by factors of the ETS family. Previous studies showed that on the one hand, in given experimental conditions, the AP-1 complex was required for ETS-1 transcriptional activity (56) and on the other hand that the recruitment by direct protein-protein interactions of the AP-1 complex by ETS-2 was increased in the presence of the EBS palindrome of the stromelysin-1 promoter (41). Hence, the observed binding cooperativity, mediated by a structural rearrangement implying the exon VII-encoded region, could play a crucial role in the optimum presentation of the molecule to its partners. These spatial and molecular events could lead to the unmasking or the formation of a specific interaction surface. This does not only concern transcriptional partners like AP-1 or CBFα2 but also general transcriptional coactivators. Indeed, CBP/p300 was shown to interact directly with ETS-1 and ETS-2 and particularly in the case of transactivation of the stromelysin-1 promoter (42, 57). More recently, Sp100 was also shown to be able to interact with ETS-1 and stimulate its transcriptional activity (58). It is also noteworthy that not only the domain comprising HI-1 and HI-2 inhibitory helices is implicated but rather the entire exon VII-encoded region. The latter includes the four serines responsible for the CaMKII-dependent phosphorylation, regulating DNA binding (50, 51), which we proved to also play a role in the cooperative binding to the EBS palindrome (Fig. 6). It also contains an SCRLTQS motif located 261–267 in the protein sequence. This motif, according to computer-predicted secondary structure of ETS-1, forms an α-helix and also contains an arginine that is resistant to tryptic digestion (60). This suggests a stable secondary structure that could be involved in the autoinhibition regulation or in protein-protein contacts.

The observed cooperative binding can be easily linked to the strategy of combinatorial transcription regulation by ETS proteins. Various works studied cooperative binding of the ETS-1 protein with transcriptional partners such as CBFα2 (30, 31), USF-1 (27), or TFE3 (28) where intermolecular contacts raise autoinhibition. In the particular topology of the head to head EBS palindrome, we propose that the two ETS-1 molecules play the role of reciprocal transcriptional partners. In addition, this view can account for the observation that ERG inhibits the ETS-2 transcriptional activation of the stromelysin-1 promoter in transient co-transfection (40). ETS-2, like ETS-1, requires the presence of both vacant EBS to overcome autoinhibition and bind efficiently to the DNA. Thus, an ERG molecule would be able to occupy one of the two EBS long enough to prevent the cooperative fixation of two ETS-2 molecules. This also suggests a differential regulation of the promoter by the two isoforms of ETS-1, p42 and p51. The latter binds cooperatively to the palindrome and achieves maximum transactivation (Fig. 7) but binds poorly to M1 or M2 mutant due to DNA binding autoinhibition. In contrast, the p42 isoform can bind efficiently to a single EBS and thus prevent access to the second EBS of the palindrome, acting as a dominant negative for the activation of the stromelysin-1 promoter or other promoters where EBS are organized in the palindrome.

We postulated that ETS-1 overcomes its autoinhibition via intermolecular contacts involving the exon VII-encoding region which would favor the rapid formation of a ternary complex. The organization of two head to head EBS distant by 4 bp on a regular B-shaped double-stranded DNA in conjunction with the spatial structure of an ETS DBD bound to DNA indicates that both ETS-1 molecules are located on the same side of the DNA, and that the inhibitory modules are facing each other. However, we were not able to evidence a direct protein-protein contact. Various techniques including cross-linking, *in vitro* GST fusion pull-down assays, or SPR experiments failed to reveal a direct protein-protein interaction (data not shown). These difficulties may have two major causes. First, the supposed interaction is DNA-dependent, requiring strict proximity and proper arrangement of the molecules. Second, the inhibitory module does not exist on its own, resulting from the packing of four distinct partners: inhibitory helices HI-1 and HI-2 located at the N terminus of the DBD, inhibitory helix H4 at the C terminus of the DBD, and helix H1 in the DBD (see Fig. 3*B*). To use an isolated exon VII peptide for *in vitro* interaction assays appears useless because its proper structure would not be obtained in absence of the C-terminal part of the protein. In this context, it is noteworthy that such an involve-

ment of the exon VII-encoded region of ETS-1 in a cooperative binding to a transcriptional partner was already encountered with CBFα2 and resulted with the same difficulty to prove direct protein-protein interaction even with such a sensitive tool as SPR (31).

The EBS palindrome with 4-bp interval between ETS-binding cores present in the stromelysin-1 promoter is not found in other known promoters of matrix metalloproteinases. Its ability to recruit, in a specific way, two ETS-1 p51 molecules to form a ETS-1·DNA·ETS-1 ternary complex via the exon VII-encoded region is inherent to the autoinhibition binding mechanism of p51. To our knowledge, it is the first time that ETS-1 was shown to be able to counteract its own autoinhibition through such a complex. The existence of such a ternary complex remains to be checked in cells expressing both stromelysin-1 and ETS-1. Given that such palindromes are found in other promoters regulated by ETS proteins, these EBS palindromes might represent a hot spot to recruit autoinhibited ETS proteins and lead to specific transcriptional complexes.

Acknowledgments—We thank Drs. J. Coll and A. Verger for stimulating discussions; Dr. D. Régnier for critical reading of the manuscript; Dr. M. Dutreix for help in using Biacore® apparatus; and N. Spruyt and S. Dequiedt for technical assistance. We are grateful to Dr. G. Buttice for providing the human stromelysin-1 promoter.

REFERENCES

1. Sternlicht M., D., and Werb, Z. (1999) in *Guidebook to the Extracellular Matrix and Adhesion Proteins* (Kreis, T., and Vale, R., eds), pp. 505–563, Oxford University Press, New York
2. Vu, T. H., and Werb, Z. (2000) *Genes Dev.* **14,** 2123–2133
3. Flannery, C. R., Lark, M. W., and Sandy, J. D. (1992) *J. Biol. Chem.* **267,** 1008–1014
4. Malemud, C. J., and Goldberg, V. M. (1999) *Front. Biosci.* **4,** D762–D771
5. Yoshiyama, Y., Asahina, M., and Hattori, T. (2000) *Acta Neuropathol.* **99,** 91–95
6. Zucker, S., Cao, J., and Chen, W. T. (2000) *Oncogene* **19,** 6642–6650
7. Nelson, A. R., Fingleton, B., Rothenberg, M. L., and Matrisian, L. M. (2000) *J. Clin. Oncol.* **18,** 1135–1149
8. Liu, Z., Ivanoff, A., and Klominek, J. (2001) *Int. J. Cancer* **91,** 638–643
9. Sternlicht, M. D., Lochter, A., Sympson, C. J., Huey, B., Rougier, J. P., Gray, J. W., Pinkel, D., Bissell, M. J., and Werb, Z. (1999) *Cell* **98,** 137–146
10. Sternlicht, M. D., Bissell, M. J., and Werb, Z. (2000) *Oncogene* **19,** 1102–1113
11. Ye, S., Whatling, C., Watkins, H., and Henney, A. (1999) *FEBS Lett.* **450,** 268–272
12. Rekdal, C., Sjottem, E., and Johansen, T. (2000) *J. Biol. Chem.* **275,** 40288–40300
13. Buttice, G., and Kurkinen, M. (1993) *J. Biol. Chem.* **268,** 7196–7204
14. Wasylyk, C., Gutman, A., Nicholson, R., and Wasylyk, B. (1991) *EMBO J.* **10,** 1127–1134
15. Maroulakou, I. G., and Bowe, D. B. (2000) *Oncogene* **19,** 6432–6442
16. Bartel, F. O., Higuchi, T., and Spyropoulos, D. D. (2000) *Oncogene* **19,** 6443–6454
17. Raouf, A., and Seth, A. (2000) *Oncogene* **19,** 6455–6463
18. Lelievre, E., Lionneton, F., Soncin, F., and Vandenbunder, B. (2001) *Int. J. Biochem. Cell Biol.* **33,** 391–407
19. Dittmer, J., and Nordheim, A. (1998) *Biochim. Biophys. Acta* **1377,** F1–F11
20. Sharrocks, A. D., Brown, A. L., Ling, Y., and Yates, P. R. (1997) *Int. J. Biochem. Cell Biol.* **29,** 1371–1387
21. Graves, B. J., and Petersen, J. M. (1998) *Adv. Cancer Res.* **75,** 1–55
22. Sharrocks, A. D. (2001) *Nat. Rev. Mol. Cell. Biol.* **2,** 827–837
23. Graves, B. J., Cowley, D. O., Goetz, T. L., Petersen, J. M., Jonsen, M. D., and Gillespie, M. E. (1998) *Cold Spring Harbor Symp. Quant. Biol.* **63,** 621–629
24. Lim, F., Kraut, N., Frampton, J., and Graf, T. (1992) *EMBO J.* **11,** 643–652
25. Skalicky, J. J., Donaldson, L. W., Petersen, J. M., Graves, B. J., and McIntosh, L. P. (1996) *Protein Sci.* **5,** 296–309
26. Jonsen, M. D., Petersen, J. M., Xu, Q. P., and Graves, B. J. (1996) *Mol. Cell. Biol.* **16,** 2065–2073
27. Sieweke, M. H., Tekotte, H., Jarosch, U., and Graf, T. (1998) *EMBO J.* **17,** 1728–1739
28. Tian, G., Erman, B., Ishii, H., Gangopadhyay, S. S., and Sen, R. (1999) *Mol. Cell. Biol.* **19,** 2946–2957
29. Kim, W. Y., Sieweke, M., Ogawa, E., Wee, H. J., Englmeier, U., Graf, T., and Ito, Y. (1999) *EMBO J.* **18,** 1609–1620
30. Gu, T. L., Goetz, T. L., Graves, B. J., and Speck, N. A. (2000) *Mol. Cell. Biol.* **20,** 91–103
31. Goetz, T. L., Gu, T. L., Speck, N. A., and Graves, B. J. (2000) *Mol. Cell. Biol.* **20,** 81–90
32. Mauviel, A. (1993) *J. Cell. Biochem.* **53,** 288–295
33. Redlich, K., Kiener, H. P., Schett, G., Tohidast-Akrad, M., Selzer, E., Radda, I., Stummvoll, G. H., Steiner, C. W., Groger, M., Bitzan, P., Zenz, P., Smolen, J. S., and Steiner, G. (2001) *Arthritis Rheum.* **44,** 266–274
34. Sun, H. B., and Yokota, H. (2001) *Bone* **28,** 303–309
35. Naito, T., Razzaque, M. S., Nazneen, A., Liu, D., Nihei, H., Koji, T., and Taguchi, T. (2000) *J. Am. Soc. Nephrol.* **11,** 2243–2255
36. Oda, N., Abe, M., and Sato, Y. (1999) *J. Cell. Physiol.* **178,** 121–132
37. Wernert, N., Gilles, F., Fafeur, V., Bouali, F., Raes, M. B., Pyke, C., Dupressoir, T., Seitz, G., Vandenbunder, B., and Stehelin, D. (1994) *Cancer Res.* **54,** 5683–5688
38. Seth, A., Robinson, L., Thompson, D. M., Watson, D. K., and Papas, T. S. (1993) *Oncogene* **8,** 1783–1790
39. Venanzoni, M. C., Robinson, L. R., Hodge, D. R., Kola, I., and Seth, A. (1996) *Oncogene* **12,** 1199–1204
40. Buttice, G., Duterque-Coquillaud, M., Basuyaux, J. P., Carrere, S., Kurkinen, M., and Stehelin, D. (1996) *Oncogene* **13,** 2297–2306
41. Basuyaux, J. P., Ferreira, E., Stehelin, D., and Buttice, G. (1997) *J. Biol. Chem.* **272,** 26188–26195
42. Jayaraman, G., Srinivas, R., Duggan, C., Ferreira, E., Swaminathan, S., Somasundaram, K., Williams, J., Hauser, C., Kurkinen, M., Dhar, R., Weitzman, S., Buttice, G., and Thimmapaya, B. (1999) *J. Biol. Chem.* **274,** 17342–17352
43. Ho, S. N., Hunt, H. D., Horton, R. M., Pullen, J. K., and Pease, L. R. (1989) *Gene* (*Amst.*) **77,** 51–59
44. Hodge, D. R., Robinson, L., Watson, D., Lautenberger, J., Zhang, X. K., Venanzoni, M., and Seth, A. (1996) *Oncogene* **12,** 11–18
45. Pio, F., Kodandapani, R., Ni, C. Z., Shepard, W., Klemsz, M., McKercher, S. R., Maki, R. A., and Ely, K. R. (1996) *J. Biol. Chem.* **271,** 23329–23337
46. Mo, Y., Vaessen, B., Johnston, K., and Marmorstein, R. (1998) *Mol. Cell* **2,** 201–212
47. Fancy, D. A., and Kodadek, T. (1999) *Proc. Natl. Acad. Sci. U. S. A.* **96,** 6020–6024
48. Fisher, R. J., Fivash, M., Casas-Finet, J., Erickson, J. W., Kondoh, A., Bladen, S. V., Fisher, C., Watson, D. K., and Papas, T. (1994) *Protein Sci.* **3,** 257–266
49. Fisher, R. J., Koizumi, S., Kondoh, A., Mariano, J. M., Mavrothalassitis, G., Bhat, N. K., and Papas, T. S. (1992) *J. Biol. Chem.* **267,** 17957–17965
50. Cowley, D. O., and Graves, B. J. (2000) *Genes Dev.* **14,** 366–376
51. Rabault, B., and Ghysdael, J. (1994) *J. Biol. Chem.* **269,** 28143–28151
52. Higashino, F., Yoshida, K., Noumi, T., Seiki, M., and Fujinaga, K. (1995) *Oncogene* **10,** 1461–1463
53. Fenrick, R., Wang, L., Nip, J., Amann, J. M., Rooney, R. J., Walker-Daniels, J., Crawford, H. C., Hulboy, D. L., Kinch, M. S., Matrisian, L. M., and Hiebert, S. W. (2000) *Mol. Cell. Biol.* **20,** 5828–5839
54. Garvie, C. W., Hagman, J., and Wolberger, C. (2001) *Mol. Cell* **8,** 1267–1276
55. Wang, H., McIntosh, L. P., and Graves, B. J. (2002) *J. Biol. Chem.* **277,** 2225–2233
56. Crawford, H. C., Fingleton, B., Gustavson, M. D., Kurpios, N., Wagenaar, R. A., Hassell, J. A., and Matrisian, L. M. (2001) *Mol. Cell. Biol.* **21,** 1370–1383
57. Yang, C., Shapiro, L. H., Rivera, M., Kumar, A., and Brindle, P. K. (1998) *Mol. Cell. Biol.* **18,** 2218–2229
58. Wasylyk, C., Schlumberger, S. E., Criqui-Filipe, P., and Wasylyk, B. (2002) *Mol. Cell. Biol.* **22,** 2687–2702
59. Nesterenko, M. V., Tilley, M., and Upton, S. J. (1994) *J. Biochem. Biophys. Methods* **28,** 239–242
60. Cowley, D. O. (2000) *Regulation of Transcription Factors ETS-1 and ETS-2 by Autoinhibition and Phosphorylation,* Ph.D. dissertation, University of Utah